NASA Technical Memorandum 106834

Cochannel and Adjacent-Channel Interference in Nonlinear Minimum-Shift-Keyed Satellite System

John Yu
Lewis Research Center
Cleveland, Ohio

March 1995

National Aeronautics and
Space Administration

Cochannel and Adjacent-Channel Interference in Nonlinear Minimum-Shift-Keyed Satellite System

John Yu
National Aeronautics and Space Administration
Lewis Research Center
Cleveland, Ohio 44135

Summary

The interference susceptibility of a serial-minimum-shift-keyed (SMSK) modulation system to an interfering signal transmitted through a satellite link with cascaded nonlinear elements was investigated through computer simulation. The satellite link evaluated in this study represented NASA's Advanced Communications Technology Satellite (ACTS) system. Specifically, nonlinear characteristics were used that had specified amplitude-modulation-to-amplitude-modulation and amplitude-modulation-to-phase-modulation transfer characteristics obtained from the actual ACTS hardware. Two measurement scenarios were analyzed: degradation of an MSK satellite link from cochannel interference and from adjacent-channel interference. Interference was evaluated in terms of the probability of bit error rate (BER) versus energy per bit over noise power density E_b/N_0.

Introduction

Modern satellite communications systems suffer from interferences emanating from various sources as a result of sharing the communications spectrum. The interference may be caused by a neighboring satellite operating at the same frequency (cochannel interference) or at a nearby frequency (adjacent-channel interference). Such interference can impair overall system performance both in the up- and downlink paths. In addition, satellite transponders (high-power amplifier (HPA) or traveling-wave-tube amplifier (TWTA)) operating near or at saturation contribute additional impairments through nonlinear distortion. In a highly spectral congested satellite system environment, it is often desirable to employ a digital modulation system where constant-envelope, continuous-phase, spectral efficiency and some immunity to nonlinear distortion generated by satellite transponders is achieved. One such modulation scheme that bears all these attributes is known as minimum-shift-keyed (MSK) modulation (ref. 1).

There are two methods of generating the MSK signal. The first method is conventional parallel implementation, where two half-sinusoid, pulse-shaped data streams are used to provide in-phase and quadrature components of the modulated carrier. The modulation is obtained by staggering the data streams, which are shifted by a one-half symbol period on quadrature carriers. The second and simpler method is serial implementation (hereinafter referred to as serial MSK or SMSK). In this approach, the MSK signal is produced from a biphase signal by filtering it with an appropriately designed linear time-invariant filter. The mathematical derivations for these two methods are presented in references 1 and 2, respectively.

This study investigated the latter method, specifically, the performance of a serial MSK modulation system over a wideband, hard-limited transponder representative of the ACTS channel in the presence of cochannel and adjacent-channel interference and additive noise. The performance is presented in terms of end-to-end system bit error rate (BER) versus the required energy per bit over noise power density E_b/N_0. A computer simulation software package called the Signal Processing Worksystem was used to estimate the BER.

The semi-analytical estimation method, which yields the fastest computation time (ref. 3), was used to calculate the BER. In this method, two assumptions are made. First, it is assumed that all system noise sources can be modeled as one equivalent noise source by using a Gaussian distribution. And second, the system is assumed to be linear at the receiver where the Gaussian noise is referenced. Thus, knowing the noise distribution to be Gaussian, the probability of bit error can be computed by using $P_e = Q[S_i/\sigma]$, where Q is the Marcum-Q function, S_i is the noiseless waveform sampled at the i^{th} sampling instant, and σ is the standard deviation of the distribution. In this way, an independent calculation is performed at each of the N sampling instants. The total probability of error over N trials is then the average of the N individual probabilities. The semi-analytic BER estimation technique is described in the next section.

System Model

The simplified block diagram of a serial MSK communications system model for interference measurement (fig. 1) has five major blocks: PN sequence generator, SMSK modulator, ACTS, SMSK demodulator, and semi-analytic BER estimator. Each is implemented by the Signal Processing Worksystem. The PN sequence generator provides pseudo-noise data streams to the SMSK modulator. Two different sets of data streams are generated for the "desired" and "interference" channels. In the serial MSK modulator structure

(fig. 2(a), from ref. 4), the incoming bit stream is modulated by a binary-phase-shift-keyed (BPSK) modulator with a carrier frequency of $f_1 = f_0 - 1/4T$. The bit stream is then passed through a bandpass conversion filter with an impulse response of

$$g(t) = \begin{cases} 2\sin(2\pi f_2 t) & 0 \le t \le T \\ 0 & \text{otherwise} \end{cases} \quad (1)$$

where $f_2 = f_0 + 1/4T$ and f_0, f_1, and f_2 are the apparent carrier, mark, and space frequencies, respectively (ref. 4). I have followed this notation throughout this paper. The key element in generating serial MSK signaling is the conversion filter.

The impulse response for the ideal conversion filter, from equation (1), can be rewritten as

$$g(t) = \begin{cases} 2\sin\left[2\pi\left(f_0 + 1/4T\right)t\right] & 0 \le t \le T \\ 0, & \text{otherwise} \end{cases}$$

and

$$g(t) = 2\cos\left[2\pi\left(f_0 + \frac{1}{4T}\right)t - \frac{\pi}{2}\right] \times \Pi\left(\frac{t}{T} - \frac{1}{2}\right) \quad (2)$$

where $\Pi(t) \triangleq 1, -1/2 \le t \le 1/2$. After mathematic manipulation, it can be shown that

$$g(t) = \mathrm{Re}\left[2e^{j2\pi\left(\frac{t}{2T} - \frac{1}{2}\right)} \times e^{j2\pi\left(f_0 - \frac{1}{4T}\right)t} \times \Pi\left(\frac{t}{T} - \frac{1}{2}\right)\right] \quad (3)$$

Equation (3) is used to generate gains for each stage of the conversion filter. The conversion filter is designed by using a simple direct-form realization of the finite impulse response filter with N samples per bit (N = 16 was used in this study). The corresponding demodulator (fig. 2(b)) is essentially the reverse operation of the modulator structure. The theoretical aspects of conversion and matched filters are discussed more thoroughly in reference 2.

The ACTS module used in this study mirrors the nonlinearity of the actual ACTS system. As shown in figure 3, the ACTS module consists of the low-pass filter and three cascaded TWT elements, providing hard-limiting effects. The three TWT elements—the intermediate-frequency (IF) amplifier, the upconverter, and the TWTA—were modeled in the same fashion by using a TWT-table module. This module is characterized by a look-up table containing amplitude-modulation-to-amplitude-modulation (AM/AM) and amplitude-modulation-to-phase-modulation (AM/PM) characteristics obtained from the ACTS hardware. The low-pass filter, which provides channel filtering, is a two-pole Butterworth type with a passband edge frequency of 3 Hz. No other transmitting-and-receiving filter exists in the system. The average complex power blocks were used to set the correct TWT backoff levels.

The system BER was calculated by a semi-analytic technique and is represented by the semi-analytic BER estimator block (fig. 4). The magnitude of input to this module represents the normalized received BPSK waveform. Hence, with the assumption of Gaussian noise in the system, the BER could be calculated from (ref. 5):

$$P_e = \left[\sqrt{\frac{2E_b}{N_0}}\right] \quad (4)$$

where P_e is the probability of bit error, E_b is the energy of the received signal, and N_0 is the noise power. Thus, as shown in figure 4, the received waveform was passed through a series of blocks so that it could be put into the form of equation (4). The resulting waveform was fed into a Marcum-Q function, where the probability that the waveform was an error was calculated by using standard normal distribution. This approach produced a statistically accurate ($\pm 7.5\times10^{-8}$) estimate of the BER as long as a statistically representative eye diagram was used and optimum sampling points were taken. The average BER was then calculated by summing all P_e values and dividing by the total number of samples received.

Two measurement scenarios were investigated in this study. The first scenario simulated cochannel interference (CCI), where the secondary channel (or interferer) is transmitted at the same frequency as the primary channel (or desired) signal. CCI can be quantified by determining the BER as a function of relative interferer power levels. In the second scenario, the interferer is transmitted at varying frequencies adjacent to the desired signal. Adjacent-channel interference (ACI) is quantified by determining the BER as a function of channel spacing. The effects of cochannel and adjacent-channel interference were measured for both the up- and downlink paths. The BER-versus-required-E_b/N_0 curve for the computer simulation baseline was established as shown in figure 5. The back-to-back measurement of the SMSK modem, denoted in the figure as "SPW ideal," closely matched the theoretical BER curve. The BER curve of ACTS transmission with no interference, denoted as "ACTS path," yielded degradation of 0.5 dB from theory at a BER of 10^{-6}.

Simulation Results for Cochannel Interference

Cochannel interference was simulated for the relatively wideband, hard-limiting transponder represented by the ACTS system. Thus, the absence of intersymbol interference

was assumed. In this study, four separate interferer power levels were used to quantify the BER: −3, −6, −10, and −20 dBc. The BER-versus-required-E_b/N_0 curves for uplink CCI (fig. 6) indicate that the uplink cochannel interferer produced virtually no BER degradation at or below −20 dBc, about 0.4 dB of degradation at −10 dBc, and about 2.0 dB at −6 dBc. As the interferer level increased above −6 dBc, the effects of cochannel interference became severe.

The downlink cochannel interference results for the four power levels (fig. 7) show that, as expected, downlink interference produced more degradation than uplink interference, except at −20 dBc, where the interferer power level was assumed to be negligible. For example, the degradation increased by 0.4 to about 0.8 dB at −10 dBc and by about 3.7 dB at −6 dBc. The degradation became severe above −6 dBc. The lower degradation with uplink interference can be attributed to small-signal suppression in the uplink transmission. That is, when two signals with unequal power are passed through a hard-limiting transponder, the signal with less power is suppressed.

Simulation Results for Adjacent-Channel Interference

Adjacent-channel interference is mainly caused by the power spectral spreading of one channel into an adjacent channel. Thus, ACI is measured as a function of channel spacing and relative power level. In this study, channel spacing was determined by the apparent carrier frequency of the SMSK modulator, which was set to 0.25 Hz. The BER-versus-required-E_b/N_0 curves for the uplink ACI spaced in the frequency domain just above the desired channel are presented in figure 8 for the four power levels. They show that interferer power levels below −10 dBc caused no measurable degradation but that the degradation was 0.2 dB at −6 dBc and 1.1 dB at −3 dBc. When the interferer power level was equal to that of the desired channel, ACI produced about 3.0 dB of degradation. Plotting the degradation at BER = 10^{-6} versus the channel spacing (fig. 9) showed that degradation flattened out when the frequency offset was larger than 1.5 Hz. In theory, the main lobe of the SMSK spectrum is 1.5 times wider than the data rate. Therefore, if the interferer channel is centered at 1.5 Hz or greater, no interference should be seen.

The downlink adjacent-channel results for four power levels (fig. 10) show no measurable degradation at any power level. In ACI the downlink performed better than the uplink because the downlink is not affected by nonlinear distortion, which only occurs in the uplink. Furthermore, the effect of the amplitude and phase nonlinearities is greater than the small-signal suppression. The less susceptibility to interference in the downlink for the ACI case is consistent with the laboratory measurements presented in reference 6. The degradation of the BER versus the channel spacing for the downlink ACI is shown in figure 11. As seen in the uplink case, the amount of degradation was significantly high as the channels are packed more closely together. Notice also that the degradation decreased until the to 1.5 Hz mark and that no measurable degradation occurred thereafter. Overall, the ACI measurement shows that interference between channels was minimal, provided that the adjacent-channel main lobes did not overlap.

Conclusions

Several cochannel and adjacent-channel interference degradation measurements of a serial-minimum-shift-keyed satellite system have been presented. These measurements were made on a computer simulation by using the ACTS mathematical model. In general, the results indicate that for cochannel interference the uplink is less susceptible to interference than the downlink because of small-signal suppression in the uplink transmission. However, for adjacent-channel interference the uplink interference produced more degradation than the downlink. This follows from the nonlinear distortion caused by the satellite transponder that occurs for the uplink interferers. Furthermore, the effect of small-signal suppression, which enhances the uplink transmission, is less than the nonlinear distortion caused by the hard-limiting transponder. It was observed that, for cochannel interference, for a bit error rate of 10^{-6} and interferer power level at −6 dBc, serial MSK performance is degraded approximately by 2.0 dB and 3.7 dB for uplink and downlink, respectively. And for the adjacent-channel interference (Δ = 1.5 Hz) at a bit error rate of 10^{-6} and interferer power level at −3 dBc, uplink interference produced 1.1 dB of degradation and there was no degradation in the downlink. These measurements have shown that the wideband, nonlinear minimum-shift-keyed satellite channel, in general, performs well in the interference envirnment.

References

1. Pasupathy, S.: Minimum Shift Keying: A Spectrally Efficient Modulation. IEEE Communications Magazine, July 1979, pp. 14–22.
2. Amoroso, F.; and Kivett, A.: Simplified MSK Signaling Technique. IEEE Trans. Commun., Apr. 1977, pp. 433–440.
3. Jeruchim, M.C.: Techniques for Estimating the Bit Error Rate in the Simulation of Digital Communication Systems. IEEE Journal on Selected Areas in Communications, vol. SAC-2, no. 1, Jan. 1984, pp. 153–170.
4. Ziemer, R.E.; Ryan, C.R.; and Stilwell, J.H.: Conversion and Matched Filter Approximations for Serial Minimum-Shift Keyed Modulation. IEEE Trans. Commun., vol. COM-30, no. 3, Mar. 1982, pp. 495–509.
5. Couch, L.W.: Digital and Analog Communication Systems. Macmillan, Inc., New York, 1987.
6. Kerczewski, R.J. and Fujikawa, G., "Interference Susceptibility Measurements for an MSK Satellite Communication Link," NASA TM–105395, 1992.

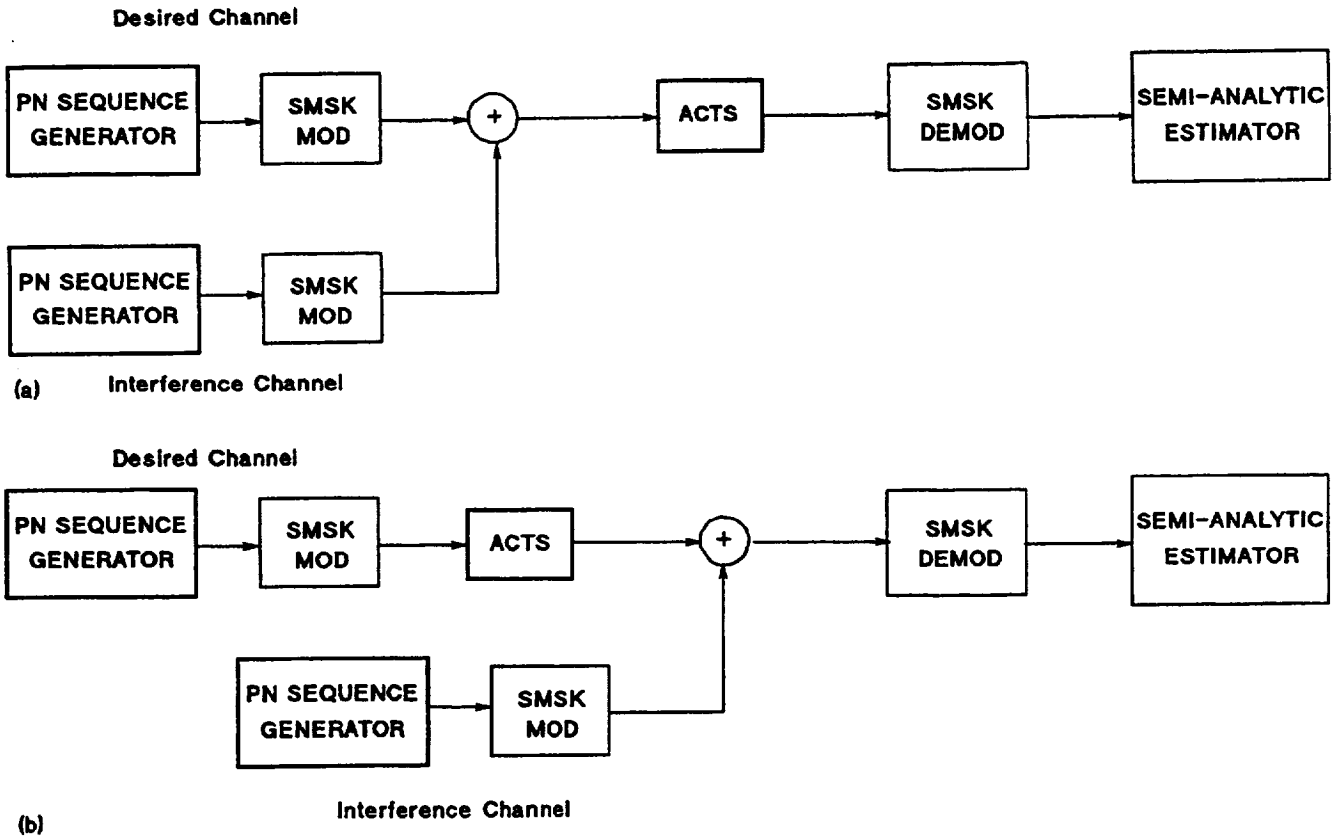

Figure 1.—System model. (a) Uplink. (b) Downlink.

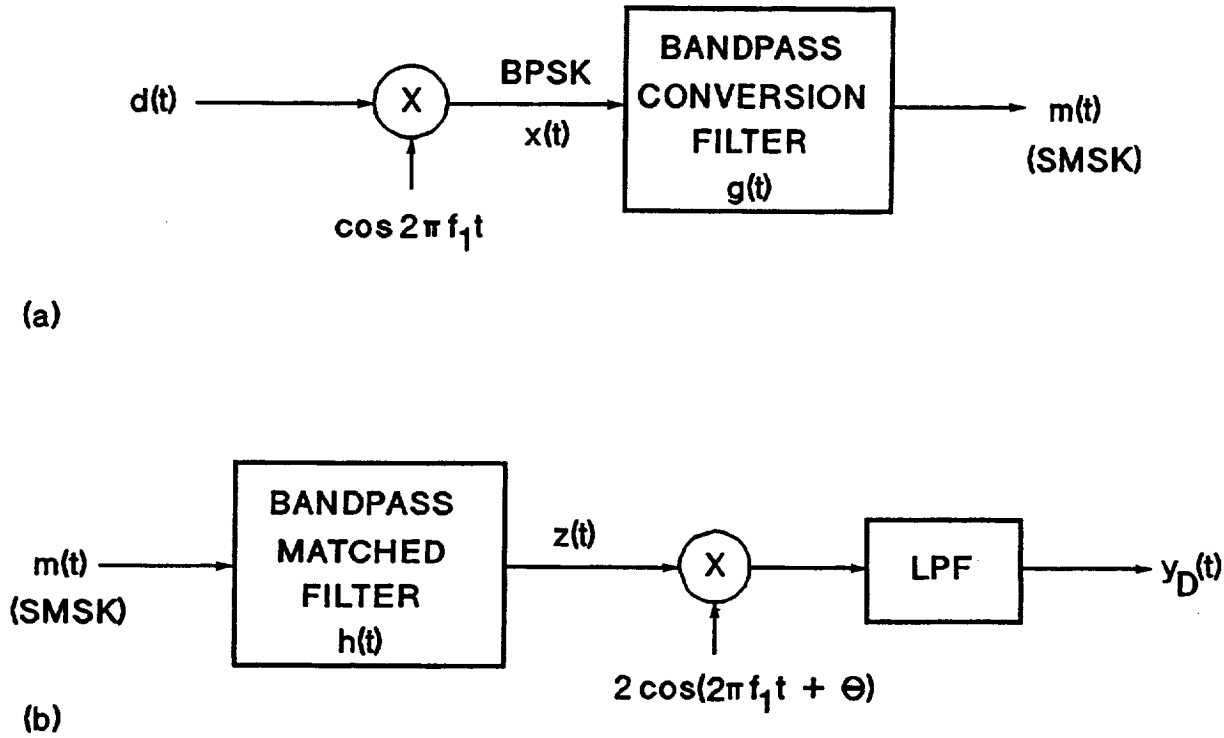

Figure 2.—Serial MSK (SMSK). (a) Modulator. (b) Demodulator.

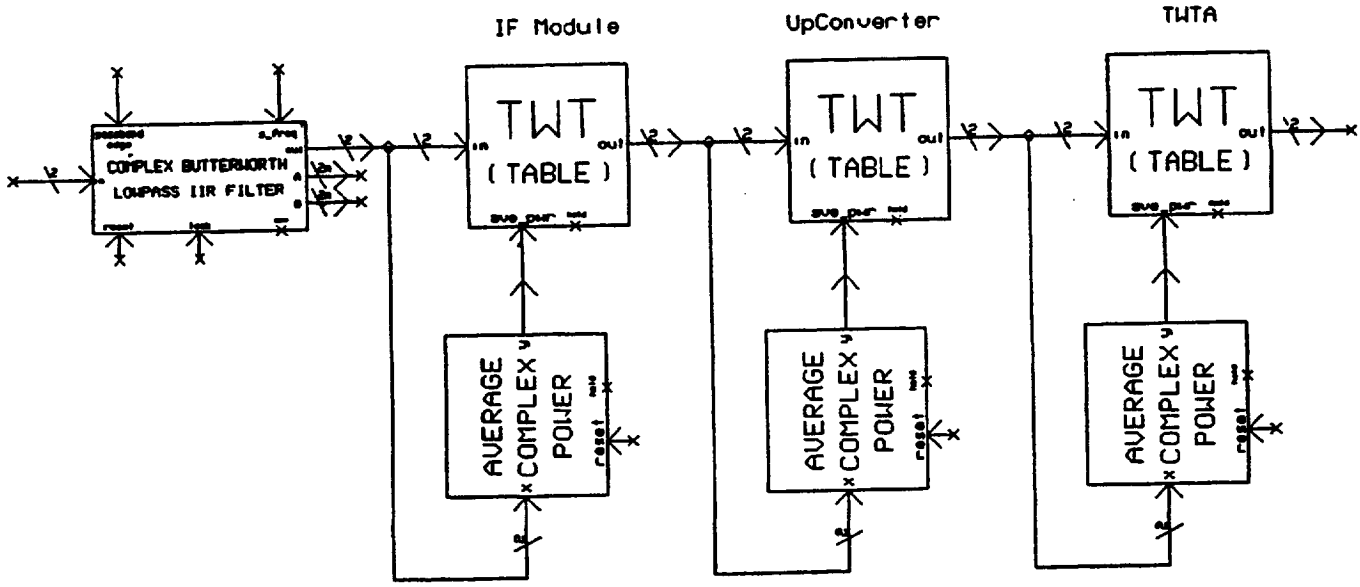

Figure 3.—ACTS model.

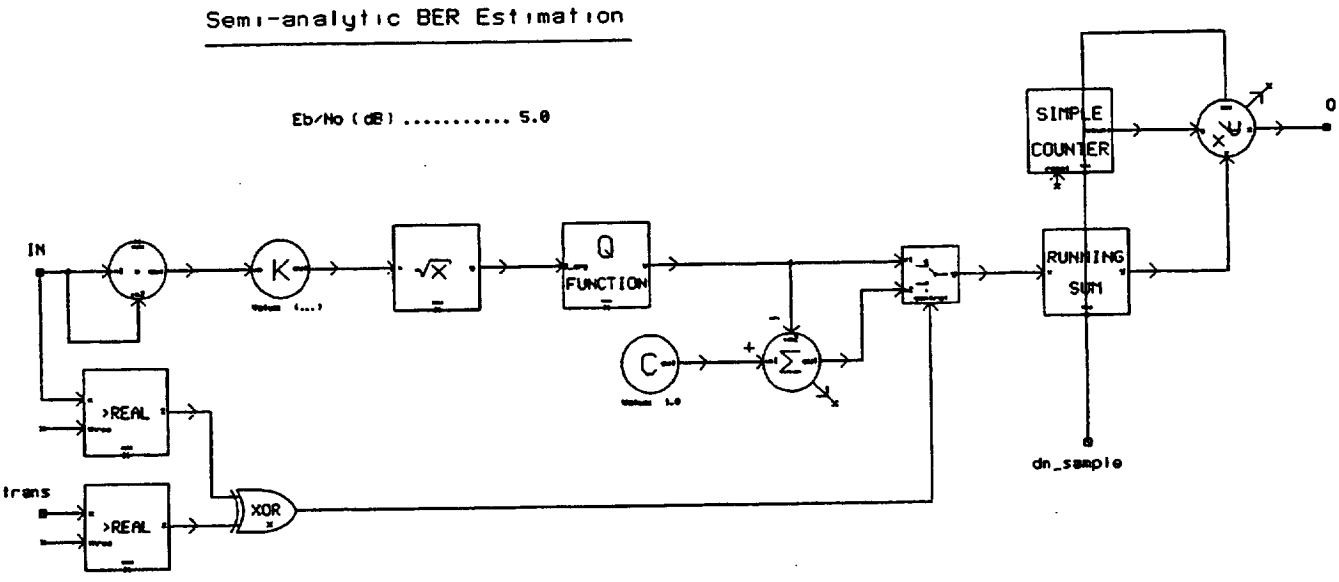

Figure 4.—Semi-analytic BER estimator.

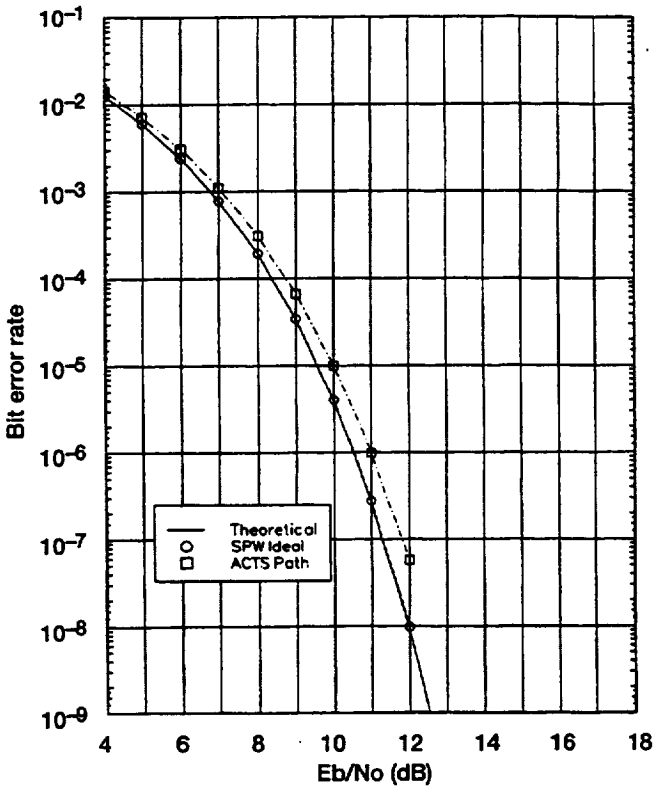

Figure 5.—SMSK transmission baseline.

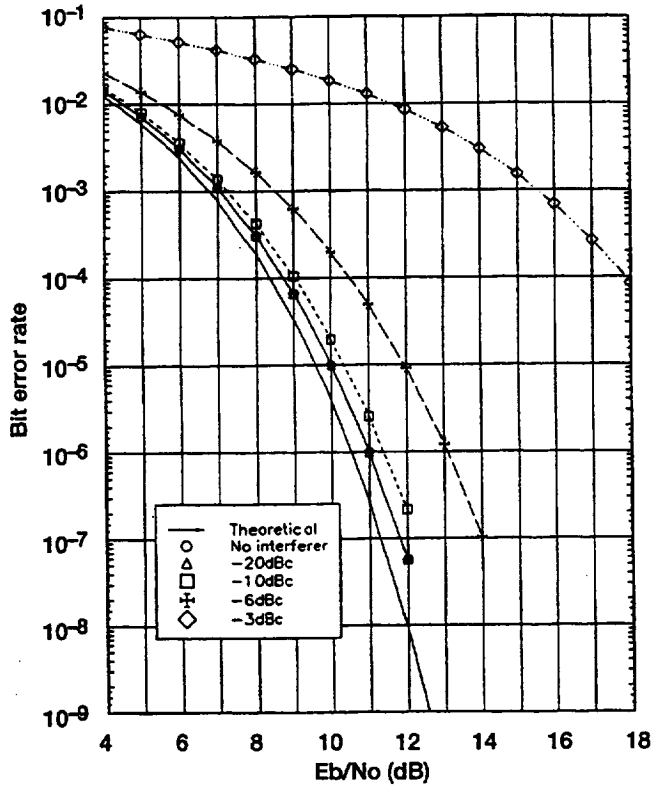

Figure 6.—Uplink cochannel interference.

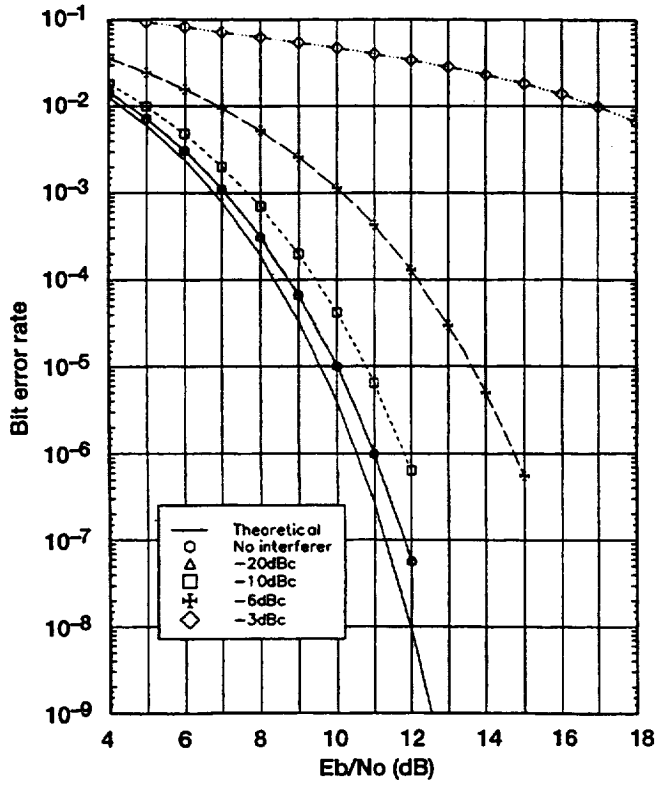

Figure 7.—Downlink cochannel interference.

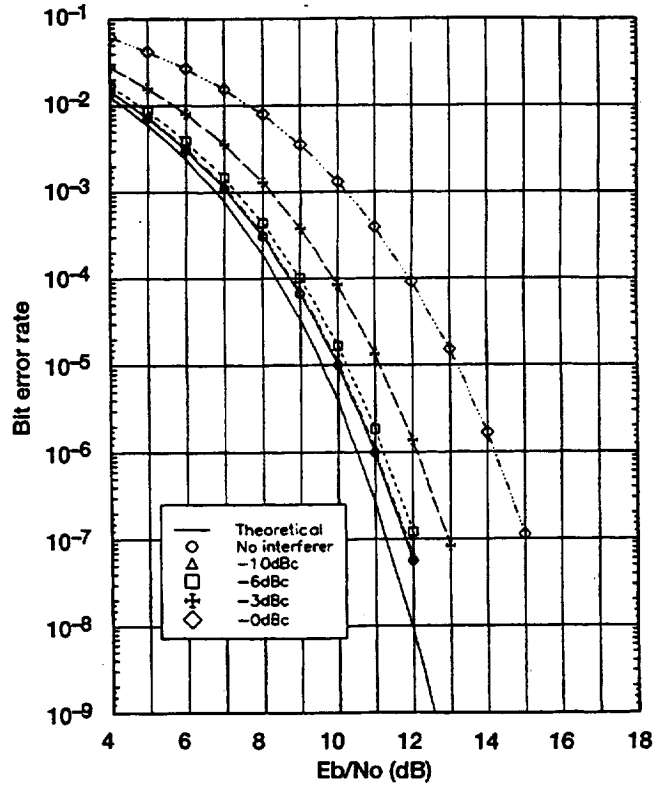

Figure 8.—Uplink adjacent channel interference ($\Delta f = 1.5$ Hz).

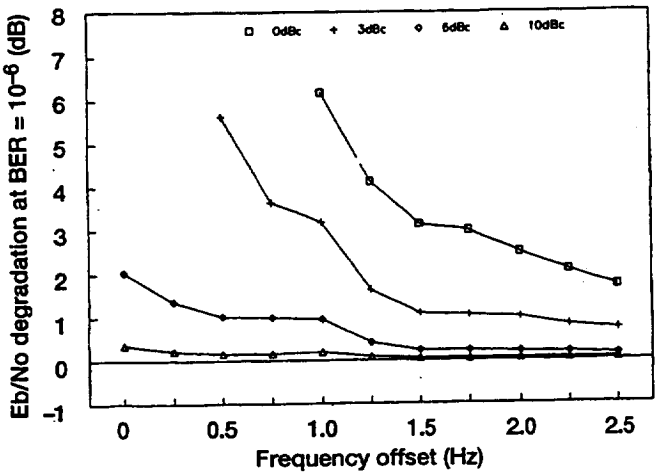

Figure 9.—Uplink BER degradation as a function of interferer frequency and relative power.

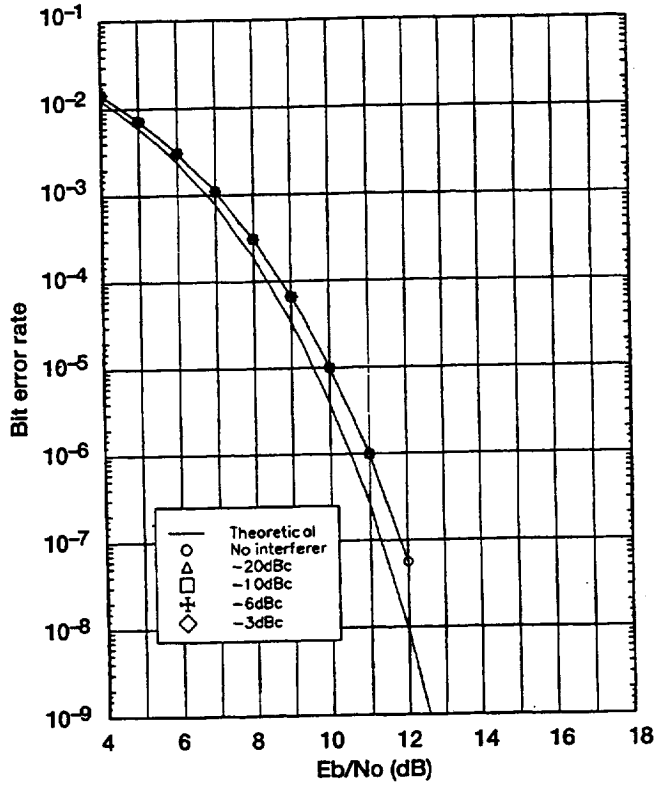

Figure 10.—Downlink adjacent channel interference ($\Delta f = 1.5$ Hz).

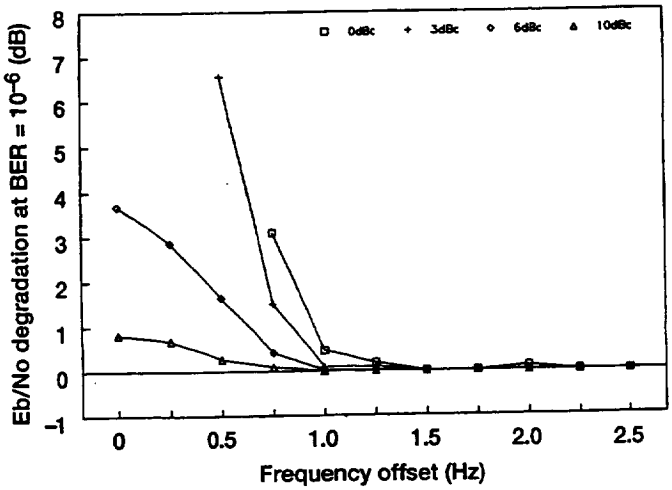

Figure 11.—Downlink BER degradation as a function of interferer frequency and relative power.

REPORT DOCUMENTATION PAGE

Form Approved
OMB No. 0704-0188

1. AGENCY USE ONLY (*Leave blank*)	2. REPORT DATE	3. REPORT TYPE AND DATES COVERED
	March 1995	Technical Memorandum

4. TITLE AND SUBTITLE

Cochannel and Adjacent-Channel Interference in Nonlinear Minimum-Shift-Keyed Satellite System

5. FUNDING NUMBERS

WU-235-01-03

6. AUTHOR(S)

John Yu

7. PERFORMING ORGANIZATION NAME(S) AND ADDRESS(ES)

National Aeronautics and Space Administration
Lewis Research Center
Cleveland, Ohio 44135-3191

8. PERFORMING ORGANIZATION REPORT NUMBER

E-9395

9. SPONSORING/MONITORING AGENCY NAME(S) AND ADDRESS(ES)

National Aeronautics and Space Administration
Washington, D.C. 20546-0001

10. SPONSORING/MONITORING AGENCY REPORT NUMBER

NASA TM-106834

11. SUPPLEMENTARY NOTES

Responsible person, John Yu, organization code 5660, (216) 433-8494.

12a. DISTRIBUTION/AVAILABILITY STATEMENT

Unclassified - Unlimited
Subject Category 32

This publication is available from the NASA Center for Aerospace Information, (301) 621-0390.

12b. DISTRIBUTION CODE

13. ABSTRACT ***(Maximum 200 words)***

The interference susceptibility of a serial-minimum-shift-keyed (SMSK) modulation system to an interfering signal transmitted through a satellite link with cascaded nonlinear elements was investigated through computer simulation. The satellite link evaluated in this study represented NASA's Advanced Communications Technology Satellite (ACTS) system. Specifically, nonlinear characteristics were used that had specified amplitude-modulation-to-amplitude-modulation and amplitude-modulation-to-phase-modulation transfer characteristics obtained from the actual ACTS hardware. Two measurement scenarios were analyzed: degradation of an MSK satellite link from cochannel interference and from adjacent-channel interference. Interference was evaluated in terms of the probability of bit error rate (BER) versus energy per bit over noise power density E_b/N_o.

14. SUBJECT TERMS

Cochannel; Adjacent-channel; Nonlinear; Minimum-shift-keyed; Satellite; Interface

15. NUMBER OF PAGES

09

16. PRICE CODE

A02

17. SECURITY CLASSIFICATION OF REPORT	18. SECURITY CLASSIFICATION OF THIS PAGE	19. SECURITY CLASSIFICATION OF ABSTRACT	20. LIMITATION OF ABSTRACT
Unclassified	Unclassified	Unclassified	